Chaos in a Small Weather Model

Aryeh Drager

Math 53: Chaos!
Professor Alex Barnett
Dartmouth College
Fall 2011

1. Introduction

It is common knowledge that the predictability of weather is limited due to the nonlinearity of atmospheric processes. Nevertheless, modern-day forecasts fall far short of the theoretical limit of deterministic predictability, estimated to be approximately two weeks (Wallace and Hobbs 301). The gap between modern-day forecasting accuracy and this theoretical limit arises from two key sources: limitations in our ability to observe the atmosphere (in order to obtain initial conditions for our atmospheric models) and limitations in the models themselves (computational and otherwise). Technological advances, such as those in remote sensing and computing power, continually serve to diminish these limitations. Researchers then face the challenge of translating technological advances into better forecasts.

One particular problem that emerges is that of determining the most useful locations for taking weather observations in order to suppress the growth of error in forecast models. In their 1998 paper, Edward N. Lorenz and Kerry A. Emanuel approach this problem by introducing a "very small model" with which to test various schemes of taking supplementary weather observations—schemes whose testing using "real-world," full-scale models would be prohibitively time-consuming. The value of this approach depends upon the similarity—at a general level—between the behavior of the "very small model" and that of full-scale, operational forecasting models.

The goal of this paper is to investigate Lorenz and Emanuel's "very small model" and to confirm several of their results regarding the model's behavior, particularly those relating to stability and chaos.

2. The Model

Unlike the larger models upon which it is based, the "very small model" has no vertical or meridional extent: it models the "weather" only at J equally-spaced sites around a single circle of latitude (see Figure 1). Mathematically, the model comprises a system of J coupled ordinary differential equations; for each $j = 1, \dots, J$, we have:

$$\frac{dX_j}{dt} = (X_{j+1} - X_{j-2})X_{j-1} - X_j + F, \quad (1)$$

where X_j, denotes the value of "some unspecified meteorological quantity, perhaps vorticity or temperature" at the j^{th} site and F is some forcing term. In order to create continuity through the entire circle of latitude, we "link" the two ends of the sequence of sites by defining $X_0 \equiv X_J$, $X_{-1} \equiv X_{J-1}$, and $X_{J+1} \equiv X_1$. All variables within the model are dimensionless, and one time unit corresponds to a real-world time of approximately five days.

3. Total Energy

Each of the J coupled ordinary differential equations contains a non-linear term, a

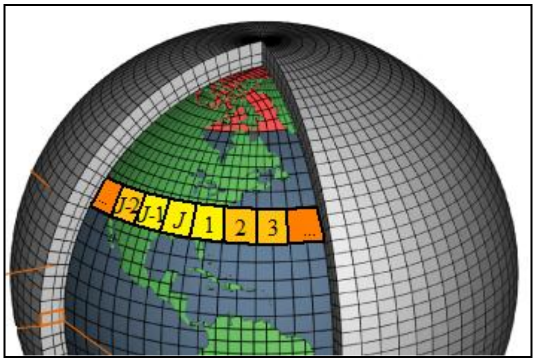

Figure 1. Visual representation of the grid of the "very small model," in orange and yellow, superimposed onto the grid of a typical full-scale atmospheric model[1]. While the full-scale model has three spatial dimensions, the "very small model" has only one.

linear term, and a constant term, intended to represent advection, dissipation, and external forcing, respectively. In order for these terms to accurately represent their intended real-world counterparts, each must affect the total energy of the system in a particular way. Terms representing advective processes must conserve total energy within the system since such real-world processes merely redistribute existing energy rather than contributing new energy or removing existing energy. Likewise, terms representing dissipative processes (such as friction) should serve to decrease the total energy of the system.

Lorenz and Emanuel define the total energy of the system as half the sum of the squares of X_j:

$$Total\ Energy \equiv \sum_{j=1}^{J} \frac{X_j^2}{2} \qquad (2)$$

We can verify that all three terms have the expected behavior by multiplying both sides of (1) by X_j and summing over all j:

$$X_j \frac{dX_j}{dt} =$$

$$\frac{d}{dt}\left(\frac{X_j^2}{2}\right) = (X_{j+1} - X_{j-2})X_{j-1}X_j - X_j^{\,2} + FX_j$$

$$\frac{d}{dt}\sum_{j=1}^{J}\left(\frac{X_j^2}{2}\right) = \frac{d}{dt}(Total\ Energy) =$$

$$\sum_{j=1}^{J}(X_{j+1} - X_{j-2})X_{j-1}X_j - \sum_{j=1}^{J} X_j^2 + \sum_{j=1}^{J} FX_j =$$

$$\sum_{j=1}^{J}(X_{j-1}X_jX_{j+1} - X_{j-2}X_{j-1}X_j) - \sum_{j=1}^{J} X_j^2 + F\sum_{j=1}^{J} X_j$$

In the final line above, we see that the first summation term, which corresponds to the advection term in (1), will equal zero, as product of each sequence of three consecutive j will be both added and subtracted exactly once. Thus, the advection term conserves total energy, as intended. The second summation term of the final line above, which corresponds to the dissipation term in (1), serves to decrease total energy, as expected. The sign of the third summation term of the final line above is not immediately obvious and depends on the sign of the sum of X_j. Nevertheless, by examining (1), we can see that the forcing term does indeed have the intended effect of "[preventing] the total energy from decaying to zero," as a strong forcing term will clearly provide a needed "boost" whenever the other terms approach zero.

4. Linear Stability Analysis

The "very small model" has what Lorenz and Emanuel refer to as an "obvious steady solution" in which all $X_j = F$. Since the stability of this equilibrium is an important feature of the system's behavior as a whole, Lorenz and Emanuel conduct a linear stability analysis of the system. In their paper, Lorenz and Emanuel provide only a three-equation outline of their analysis before reporting their results. In this section, I set out to provide the missing steps and ultimately confirm the res-

[1] Image modified from http://celebrating200years.noaa.gov/breakthroughs/climate_model/AtmosphericModelSchematic.png using Microsoft Paint.

ults of this analysis.

Let us begin by perturbing each X_j a small distance ε_j away from the steady state in which each $X_j = F$. Then, we can represent each X_j as:

$$X_j = F + \varepsilon_j, \quad (3)$$

Then by substituting (3) into (1), we obtain:

$$\frac{d}{dt}(F+\varepsilon_j) = (F+\varepsilon_{j+1} - F - \varepsilon_{j-2})(F+\varepsilon_{j-1}) - F - \varepsilon_j + F \quad (4)$$

$$\frac{dF}{dt} + \frac{d\varepsilon_j}{dt} = (\varepsilon_{j+1} - \varepsilon_{j-2})(F+\varepsilon_{j-1}) - \varepsilon_j \quad (5)$$

$$\frac{d\varepsilon_j}{dt} = (\varepsilon_{j+1} - \varepsilon_{j-2})(F+\varepsilon_{j-1}) - \varepsilon_j \quad (6)$$

$$\frac{d\varepsilon_j}{dt} = F\varepsilon_{j+1} - F\varepsilon_{j-2} + \varepsilon_{j-1}\varepsilon_{j+1} - \varepsilon_{j-2}\varepsilon_{j-1} - \varepsilon_j \quad (7)$$

$$\frac{d\varepsilon_j}{dt} \approx F(\varepsilon_{j+1} - \varepsilon_{j-2}) - \varepsilon_j \quad (8)$$

In going from (4) to (5), we remove several Fs that cancel, and we split the time derivative into two terms. In going from (5) to (6), we remove the time derivative of F because F is a constant. In going from (6) to (7), we expand the product of binomials in (6). Finally, in going from (7) to (8), we disregard terms of $O(\varepsilon^2)$ since all ε_j are very small. The result (8) is equivalent to equation (4) in Lorenz and Emanuel.

Next, we rewrite each ε_j as the sum:

$$\varepsilon_j = \sum_k p_k e^{ikj} \quad (9)$$

Similarly, we also write:

$$\varepsilon_{j-2} = \sum_k p_k e^{ik(j-2)} = \sum_k p_k e^{ikj} e^{-2ik} \quad (10)$$

$$\varepsilon_{j+1} = \sum_k p_k e^{ik(j+1)} = \sum_k p_k e^{ikj} e^{ik} \quad (11)$$

We now substitute expansions (9), (10), and (11) into (8). For each k, we now have:

$$\frac{d}{dt}(p_k e^{ikj}) = F(p_k e^{ikj} e^{ik} - p_k e^{ikj} e^{-2ik}) - p_k e^{ikj} \quad (12)$$

Canceling a common factor of e^{ikj} and factoring out the p_k on the right-hand side of (12) then yields the following differential equation for p_k, the coefficients that govern the growth of perturbations ε_j:

$$\frac{dp_k}{dt} = [(e^{ik} - e^{-2ik})F - 1]p_k \quad (13)$$

This result is identical to equation (6) in Lorenz and Emanuel.

The solution to this differential equation is:

$$p_k(t) = Ce^{[(e^{ik} - e^{-2ik})F - 1]t} \quad (14)$$

Thus, the coefficients p_k, and thus the perturbations ε_j themselves, will grow with time when:

$$\mathrm{Re}[F(e^{ik} - e^{-2ik}) - 1] > 0, \textit{ i.e.,} \quad \mathrm{Re}[F(e^{ik} - e^{-2ik})] > 1 \quad (15)$$

Similarly, perturbations ε_j will decay with time for:

$$\mathrm{Re}[F(e^{ik} - e^{-2ik}) - 1] < 0, \textit{ i.e.,} \quad \mathrm{Re}[F(e^{ik} - e^{-2ik})] < 1 \quad (16)$$

Using Euler's formula, we find that:

$$e^{ik} - e^{-2ik} = \cos(k) + i\sin(k) - \cos(-2k) - i\sin(-2k) \quad (17)$$

$$e^{ik} - e^{-2ik} = \cos(k) + i\sin(k) - \cos(2k) + i\sin(2k) \quad (18)$$

$$\mathrm{Re}(e^{ik} - e^{-2ik}) = \cos(k) - \cos(2k) \quad (19)$$

In going from (17) to (18), I rearrange minus signs using the fact that cosine is an even function and sine is an odd function. Combining (15) and (19), we obtain the result that the steady state is unstable if for some k, we have:

$$F[\cos(k) - \cos(2k)] > 1 \quad (20)$$

If we restrict F to positive values, we then find that, since the maximum value of $\cos(k) - \cos(2k)$ on $[-\pi, \pi]$ is 9/8 (which occurs at $k = \cos^{-1}(1/4) \approx 1.318$), the steady state is unstable—with respect to waves of length $2\pi/1.318 \approx 4.767$ times the distance between adjacent sites in the model—for $F > 8/9$.

Thus, if we use a model in which $J = 40$, whose divisors include both 4 and 5, we can expect wavenumber-8 and wavenumber-10 components to be among the first to appear as F increases. For waves of length 5 units, we have $\cos(2\pi/5) - \cos(4\pi/5) \approx 1.118$, and so we can expect wavenumber-8 components to appear when F exceeds $1/1.118 \approx 0.894$. Similarly, for waves of length 4 units, we have $\cos(2\pi/4) - \cos(4\pi/4) = 1$, and so we can expect wavenumber-10 components to appear when F exceeds 1 (in addition to the dominating wavenumber-8 components). These results agree with the findings of Lorenz and Emanuel.

5. Numerical Solution of Model

In the attached code, finddxdt.m and MATH53projectmodel.m, I have constructed Lorenz and Emanuel's "very small model" for $J = 40$ and $F = 8$. In order to be consistent with Lorenz and Emanuel's numerical documentation of the model, I have opted to use a fourth-order Runge-Kutta scheme, as introduced in Prof. Simon Shepherd's ENGS 91 class on October 28th, 2011.

Figure 2 shows that as time step size decreases by a factor of 10, error decreases by a factor of 10^4, in agreement with the expected

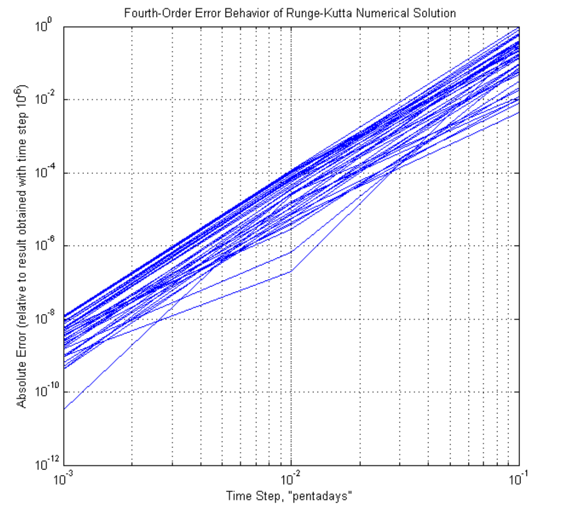

Figure 2. Illustration of fourth-order error behavior of Runge-Kutta numerical solution to time $t = 1$ for $J = 40$ and $F = 8$ with initial conditions $X_{j \neq 20} = 8$ and $X_{20} = 8.008$. The 40 lines plotted above correspond to errors recorded at the 40 sites within the model. As expected, the slope of the log-log plot is approximately equal to 4, indicating fourth-order error behavior.

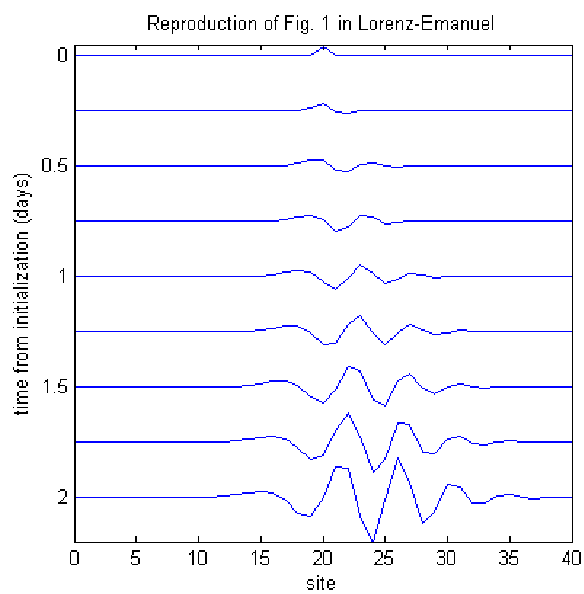

Figure 3. Illustration of the growth of a small pertubation away from the steady-state solution in which $X_j = 8$ for all j. Initial conditions as in Figure 2. Temporal spacing on the y-axis is 0.25 days; the vertical scale for perturbations away from 8 units is 0.05 units for every quarter-day. The solution obtained here appears to match that obtained in Lorenz and Emanuel's Figure 1 to fairly good precision.

error behavior for the fourth-order Runge-Kutta scheme.

My first numerical experiment was to verify the results of the linear stability analysis conducted earlier. Figure 3 shows the evolution of a 0.1% perturbation of the initial value of X_{20} away from the steady-state value F for F = 8 (much larger than the critical value of approximately 0.894). As expected, the perturbation grows with time, and by the end of the two days of perturbation evolution displayed in Figure 3, waves of length 4 and 5 units come to dominate, as expected.

Figure 4 more colorfully depicts the behavior of the system for the same initial conditions as in Figure 2 and Figure 3, this time for a total duration of three “pentadays” (fifteen days). Here, we see that after approximately one “pentaday” (33 iterations), the relative homogeneity of the system (with $X_j \approx 8$ everywhere) rather violently collapses before settling into a series of waves that tend to remain within the range −5 to 8 and appear to be dominated by wavenumber-8.

6. Quantifying Chaotic Behavior

In order to quantify a system’s sensitive dependence on initial conditions, it is useful to calculate the system’s Lyapunov exponents. In the case of Lorenz and Emanuel’s “very small model,” calculating the system’s Lyapunov exponents is a non-trivial task, as the system will have J Lyapunov exponents. In MATH53projectLyapunov.m and its associated functions, I have implemented the “Gram-Schmidt”/“QR Decomposition” numerical method for determining Lyapunov exponents discussed in Prof. Alex Barnett’s MATH 53 course on November 3rd, 2011 and November 15th, 2011.

The implementation of this method requires taking the Jacobian derivative of the system of equations represented in (1). After careful calculation of the partial derivatives of (1) with respect to each j, we obtain, for

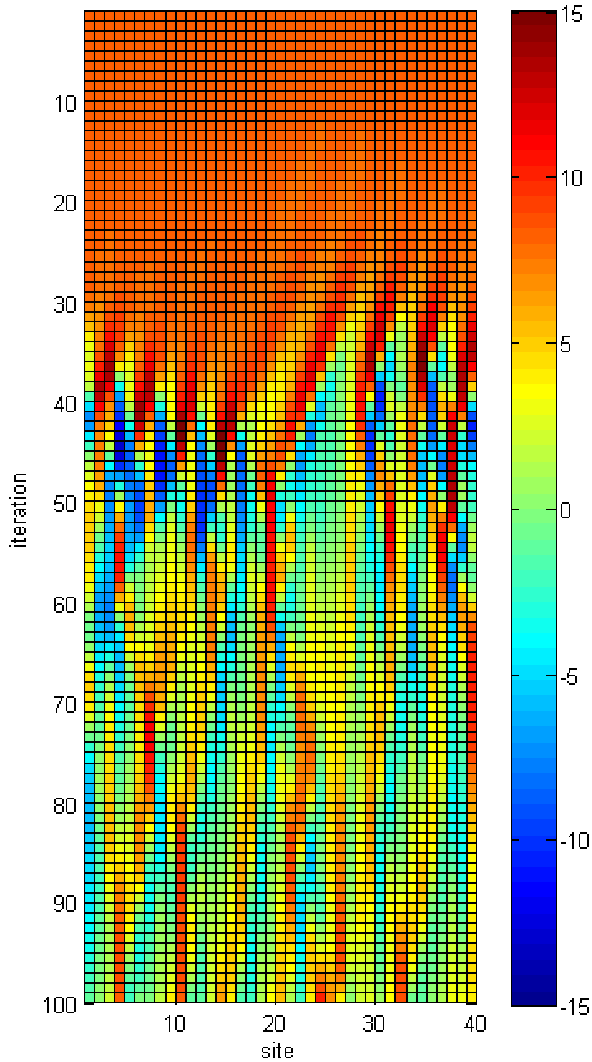

Figure 4. Illustration of the growth of the same small perturbation as in Figure 2 and Figure 3 over the course of several days. The time between plotted iterations is 0.03 “pentadays,” and the colors represent the value of each X_j at each iteration. Plot type suggested by Prof. Alex Barnett.

J = 40, the following result:

$$\vec{D}\vec{f}(\vec{X}) = \begin{bmatrix} -1 & X_{40} & & & & & -X_{40} & X_2 - X_{39} \\ X_3 - X_{40} & -1 & X_1 & & & & & -X_1 \\ -X_2 & X_4 - X_1 & -1 & X_2 & & & & \\ & -X_3 & X_5 - X_2 & -1 & X_3 & & & \\ & & \ddots & \ddots & \ddots & \ddots & & \\ & & & -X_{37} & X_{39} - X_{36} & -1 & X_{37} & \\ & & & & -X_{38} & X_{40} - X_{37} & -1 & X_{38} \\ X_{39} & & & & & -X_{39} & X_1 - X_{38} & -1 \end{bmatrix} \quad (21)$$

(21) is computed numerically in findDfdt.m. We find the Jacobian for use in Lyapunov exponent calculations by solving the following differential equation numerically:

$$\frac{dJ_t}{dt} = \vec{D}\vec{f}(\vec{X}(t)) \cdot J_t, \quad (22)$$

where J_t, the time-t Jacobian, is evolved starting from the $J \times J$ identity matrix. In order to evaluate (22) numerically using a fourth-order Runge-Kutta method within the time-t map (time1map.m), it was necessary to evolve X_j with double the temporal resolution than would have otherwise been used in order to provide mid-time step values of X_j.

After adapting the code provided by Prof. Barnett, lyapflow.m, to make it compatible with our reconstruction of Lorenz and Emanuel's "very small model," we are finally able to compute the system's Lyapunov exponents. For $J = 40$ and $F = 8$, using a time-1 pentaday map over 500 loops of 15 iterations per loop, we obtain the following Lyapunov exponents:

$h_1 = 1.6525$	$h_{21} = -0.80096$
$h_2 = 1.4156$	$h_{22} = -0.9023$
$h_3 = 1.2131$	$h_{23} = -1.0058$
$h_4 = 1.0570$	$h_{24} = -1.1124$
$h_5 = 0.91558$	$h_{25} = -1.2199$
$h_6 = 0.78841$	$h_{26} = -1.3279$
$h_7 = 0.64977$	$h_{27} = -1.4436$
$h_8 = 0.54069$	$h_{28} = -1.5795$
$h_9 = 0.41951$	$h_{29} = -1.7090$
$h_{10} = 0.30754$	$h_{30} = -1.8767$
$h_{11} = 0.20827$	$h_{31} = -2.0432$
$h_{12} = 0.094495$	$h_{32} = -2.2482$
$h_{13} = 0.00068191$	$h_{33} = -2.4831$
$h_{14} = -0.090461$	$h_{34} = -2.7542$
$h_{15} = -0.17638$	$h_{35} = -3.1114$
$h_{16} = -0.28310$	$h_{36} = -3.4972$
$h_{17} = -0.38582$	$h_{37} = -3.8747$
$h_{18} = -0.47925$	$h_{38} = -4.2170$
$h_{19} = -0.59928$	$h_{39} = -4.5073$
$h_{20} = -0.69425$	$h_{40} = -4.8398$

Thus we have thirteen positive Lyapunov exponents, the largest of which is $h_1 = 1.6525$. To find the doubling time associated with this Lyapunov exponent, we solve the equation:

$$e^{1.6525t} = 2 \quad (23)$$

Solving (23), we find:

$$1.6525t = \ln(2)$$

$$t = \frac{\ln(2)}{1.6525} = 0.4195$$

Thus the largest Lyapunov exponent is associated with a doubling time of 0.4195 pentadays, or approximately 2.1 days. Both the number of positive Lyapunov exponents and the value of the largest Lyapunov exponent agree with the results obtained by Lorenz and Emanuel.

Varying the value of F yields the following results:

F	**Number of h > 0**	**h_1**
6	10	0.9441
8	13	1.6525
10	14	2.2716
12	15	2.8116
20	16	4.7016

7. Conclusions

The goal of this project was to investigate Lorenz and Emanuel's "very small model" and to replicate some of their findings regarding the behavior of the system, particularly those regarding stability and chaotic behavior.

After confirming Lorenz and Emanuel's claims regarding the relationship between various terms within the model's differential equations and the system's total energy, we set out to examine the model itself. Linear stability analysis confirmed that the "obvious steady solution" becomes unstable as F increases beyond 0.894 and yielded the prediction that perturbation growth would be dominated by waves five "sites" in length in the case of $J = 40$.

We then shifted from pencil-and-paper analysis to numerical analysis using a fourth-order Runge-Kutta scheme. Numerical experiments successfully reproduced the perturbation growth observed by Lorenz and Emanuel, and Matlab's plotting capabilities were used to display the model's output in a more visually engaging format.

Finally, we used a"Gram-Schmidt"/"QR Decomposition" method to numerically estimate the Lyapunov exponents of the model for various amounts of forcing. The results were consistent with the observations reported by Lorenz and Emanuel.

Indeed, for large enough amounts of forcing, we conclude that Lorenz and Emanuel's "very small model" does exhibit the qualities, such as sensitive dependence on initial conditions and accurate (though quite general) representations of key atmospheric processes, requisite to serving as a useful tool for experimenting with various schemes of data assimilation and gaining insight into the behavior of the larger atmospheric models it was designed to approximate.

8. Acknowledgements

Many thanks to Prof. Alex Barnett for two incredibly engaging courses in the past two terms I've had at Dartmouth, as well as for providing encouragement and ideas throughout the process of completing this project.

9. References

1. E. N. Lorenz and K. A. Emanuel, "Optimal sites for supplementary weather observations: Simulation with a small model," J. Atmos. Sci. **55**, 399 (1998).

2. K.T. Alligood, T. D. Sauer, J. A. Yorke. Chaos: An Introduction to Dynamical Systems. (Springer-Verlag, New York, 1996)

3. Wallace, J. M., and P. V. Hobbs (2006): Atmospheric Science, An Introductory Survey, 2nd edition, Academic Press.